Electrochimica Acta 539 (2025) 147054

Contents lists available at ScienceDirect

Electrochimica Acta

journal homepage: www.journals.elsevier.com/electrochimica-acta

Functional electrolytes: Study of electrolyte for lithium-ion battery using benzene ring-containing methanesulfonate esters as additives

Keitatsu Miura [a], Yanko Marinov Todorov [b], Masaki Deguchi [c], Koji Abe [a,b,*]

[a] Graduate School of Sciences and Technology for Innovation, Yamaguchi University, 2-16-1 Tokiwadai, Ube, Yamaguchi 755-8611, Japan
[b] Organization for Research Initiatives, Yamaguchi University, 2-16-1 Tokiwadai, Ube, Yamaguchi 755-8611, Japan
[c] Panasonic Energy Co., Ltd., 1-1 Matsushita-cho, Moriguchi, Osaka 570-8511, Japan

ARTICLE INFO

Key words:
Electrolyte
Additive
Solid electrolyte interphase
Methanesulfonate esters
Benzene ring-containing compounds

ABSTRACT

With the announcement of functional electrolytes in 1999, the concept of adding around 1 to 3 wt% additives to the electrolyte to improve the performance of lithium-ion batteries (LIBs) has become widely used worldwide. In our laboratory, we have been investigating the use of methanesulfonate esters with double or triple bonds as additives to form the solid electrolyte interphase (SEI) of the anode. In this work, we investigated methanesulfonate esters with various substituents introduced into the benzene ring, which have currently not received much attention. As a result, we found that the introduction of a fluorine (F) atom is beneficial, and methanesulfonate esters containing pentafluorobenzene or trifluoromethyl benzene groups show an excellent cycling performance even when added in very low amounts of 0.5 wt% or less.

1. Introduction

In recent years, lithium-ion batteries (LIBs) have been increasingly used not only as a power source for portable devices, such as smartphones, tablets, and notebook PCs, but also for power systems in electric vehicles (EVs) and power tools, and as stationary power sources for energy storage systems (ESS). Since 1999, when the “functional electrolyte” was proposed, in which an additive of 1 to 3 wt % is intentionally decomposed prior to the decomposition of the main solvent in the electrolyte to control the solid electrolyte interphase (SEI) on the graphite anode [1,2], interest in additives that most effectively improve the LIB performance has dramatically increased [3–8].

In modern high-capacity cells with limited space for the electrolyte, an electrolyte containing large amounts of additives may ”deplete the electrolyte” after additive decomposition, causing lithium dendrite formation. Conversely, if an SEI can be formed with a small amount of additive (0.5 wt % or less), the electrolyte will not be depleted after the decomposition of the additive, and the increase in cell impedance will be suppressed and cycling performance will be improved. In this context, an increasingly important issue for the electrolyte is the control of the solid electrolyte interphase (SEI) of the graphite anode [9,10]. In order to achieve the extremely thin SEI, it is essential to research new electrolyte additives related to graphite surface modification.

Recalling the technological transition of the electrolyte, the propylene carbonate (PC) solvent was used as the main solvent for LIBs in the early 1990s with the hard carbon anode because it has a slightly higher oxidation stability than the ethylene carbonate (EC) solvent and has a melting point of −49 °C. However, when the anode was replaced from hard carbon to graphite, it was found that graphite exfoliation occurred and the battery did not work. Therefore, the electrolyte of the LIBs with the graphite anode is no longer the PC solvent, but the EC solvent with a melting point of 37 °C is now used as the electrolyte. Since the viscosity increase caused by the EC solvent reduces the transfer rate of lithium ions, a “low viscosity solvent”, such as dimethyl carbonate (DMC), is generally used in combination with the EC solvent. However, since DMC has a melting point of 3 °C, the EC/DMC electrolyte solidifies at −20 °C. Therefore, the EC solvent is mixed with asymmetric chain carbonates, such as ethyl methyl carbonate (EMC) or some of the EC solvent is replaced with the PC solvent.

Under such circumstances, the challenge was to add additives to the PC-based electrolytes to make them usable even with graphite anodes. In 1998, the group of C. Wang and Yoshio et al. succeeded in suppressing the co-intercalation of the PC solvent by adding 2 wt % 1,3-benzodioxol-2-one (also known as catechol carbonate, $C_6H_4CO_3$), a carbonate with a benzene ring [11]. In addition, in 2001, the group of S.-K. Jeong and Z. Ogumi et al. found that PC-based electrolytes with 3 wt % vinylene

* Corresponding author.
E-mail address: abekoji@yamaguchi-u.ac.jp (K. Abe).

https://doi.org/10.1016/j.electacta.2025.147054
Received 30 May 2025; Received in revised form 19 July 2025; Accepted 30 July 2025
Available online 5 August 2025

carbonate (VC), fluoroethylene carbonate (FEC), and ethylene sulfite (ES) suppressed the co-intercalation of the PC solvent as well as direct solvent decomposition on the surface of the graphite anode [12].

Therefore, we began searching for other compounds, such as carbonate compounds with terminal vinyl (-CH═CH_2) or allyl groups (-CH_2CH═CH_2) [13]. However, it was found that vinyl groups, such as vinyl acetate and vinyl adipate, have excellent cycling performances but poor chemical stability due to the influence of the Lewis acid, $LiPF_6$, in the electrolyte. When the vinyl group was replaced with an allyl group, the chemical stability improved, but the cycling performance was found to be worse than that of the vinyl group. In particular, since esters or carbonates evolve gases during reductive decomposition, we replaced them with methanesulfonates. It was then found that propargyl methanesulfonate ($CH_3SO_3CH_2C{\equiv}CH$, PMS), in which the allyl group was replaced by a triple bonded propargyl group (-$CH_2C{\equiv}CH$), showed a good cycling performance [14,15]. Subsequently, electrolytes containing PMS as an additive have been actively investigated by other researchers for electrolyte/electrode interface and mechanism analysis [16–20].

Thus, in a previous work, unsaturated structures, such as vinyl, allyl, and propargyl groups, and benzene rings with conjugated double bonds, such as catechol carbonate, have been researched as SEI-forming additives. We reported in 2002 that pentafluorophenyl methanesulfonate (PFPMS), in which all the hydrogen groups of the benzene ring were converted to fluorine (F) groups, also showed an excellent cycling performance in LIBs with graphite anodes when added in small amounts to PC-based electrolytes [21]. In 2018, the T. Yan and J. Nan et al. group also compared the addition of 1.0 wt % PFPMS with 1.0 wt % vinylene carbonate (VC) based on DFT calculations and electrochemical and TEM analyses [22]. They suggested that stable interfacial films were formed on both the $LiNi_{0.5}Co_{0.2}Mn_{0.3}O_2$ (NCM523) cathode and the graphite anode surfaces. They found a cathode electrolyte interphase (CEI) on NCM523 and an SEI on graphite leading to an improved cycling performance and reduced cell impedance. Other similar additives, methanesulfonates containing cyclic rings, such as cyclopentyl methanesulfonate and cyclohexane-1,2-diyl dimethanesulfonate, are known to inhibit the cell impedance increase [23].

In this work, we focused on methanesulfonates with a conjugated double bond benzene ring, which are chemically more stable than vinyl groups, and attempted to introduce various substituents to the benzene ring. The results were then compared to PFPMS and FEC.

2. Experimental

2.1. Chemical materials

Phenyl methanesulfonate (MSP), pentafluorobenzene (1X), perfluorobiphenyl (1Y), trifluoromethyl benzene (2X), and 4,4′-bis(trifluoromethyl)biphenyl (2Y) were purchased from Tokyo Chemical Industry (TCI) Co., Ltd. Battery grade fluoroethylene carbonate (FEC) and 2,3,4,5,6-pentafluorophenyl methanesulfonate (23456F) were purchased from the MU Ionic Solutions Corporation, controlled to H_2O: <10 ppm. All of the raw phenol compounds for the additives were selected from available inexpensive reagents. 2-Fluorophenyl methanesulfonate (2F), 3-fluorophenyl methanesulfonate (3F), 4-fluorophenyl methanesulfonate (4F), 2,6-difluorophenyl methanesulfonate (26F), 2,4-difluorophenyl methanesulfonate (24F), 3,4,5-trifluorophenyl methanesulfonate (345F), 2-(trifluoromethyl) phenyl methanesulfonate (2CF_3), 3-(trifluoromethyl) phenyl methanesulfonate (3CF_3), 4-(trifluoromethyl) phenyl methanesulfonate (4CF_3), 3,5-bis(trifluoromethyl) phenyl methanesulfonate (35CF_3), 2-cyanophenyl methanesulfonate (2CN), 2-nitrophenyl methanesulfonate (2NO_2), 2-methoxyphenyl methanesulfonate (2OCH_3), and lithium pentafluorophenoxide (1Z) were synthesized by common methods. They were stored over 4A molecular sieves (MS4A). The 1 M $LiPF_6$ PC/DMC=1/2 (v/v) and 1 M $LiPF_6$ EC/DMC=1/2 (v/v) electrolytes, controlled to H_2O<10 ppm and HF<30 ppm, were also purchased from the MU Ionic Solutions Corporation.

All the synthetic methods for the additives were common and typical. The typical isolation methods for each of the liquid and solid additives are shown below.

2.1.1. Synthesis of 2-fluorophenyl methanesulfonate (2F)

As a typical synthesis in which the purification method is distillation, we describe the preparation of 2F as an example. A 4.21 g (0.0368 mol) sample of purity 98 % 2-fluorophenol and 3.91 g (0.0384 mol) triethylamine were added to 25cm^3 of ethyl acetate and kept at 25 °C using a water bath. To this solution, 4.47 g (0.0386 mol) of 99 % methanesulfonyl chloride was slowly dropwise added. To complete the reaction, the temperature was raised to 40 °C. After 60 min, the reaction was stopped, and after washing twice with water, the ethyl acetate layer was distilled off under reduced pressure using a rotary evaporator. The 2F layer product was then purified (at 136 °C/2.0 kPa) in a distillation unit and the GC purity of 2F was 99.9 %. The 2F was made to H_2O <10 ppm by MS4A addition.

2.1.2. Synthesis of 3,5-bis(trifluoromethyl)phenyl methanesulfonate (35CF_3)

As a typical synthesis in which the purification method is crystallization, we describe the 35CF_3 as an example. The synthetic process for 35CF_3 was the same as 2F in *Section 2.1.1* up to the point where the product was distilled off under reduced pressure using a rotary evaporator. The resulting 35CF_3 solid was recrystallized using DMC, filtered, and any residual DMC was vacuum removed. The GC purity of 35CF_3 was 99.5 %. The solid 35CF_3 did not undergo dehydration with MS4A.

2.1.3. Synthesis of lithium pentafluorophenoxide (1Z)

1Z was synthesized by a simple neutralization reaction with lithium hydroxide monohydrate (LiOH・H_2O) and pentafluorophenol (C_6F_5OH). A solution of 1.03 g (0.024 mol) of LiOH・H_2O in 30 mL of ethanol was dropwise mixed with a solution of 3.70 g (0.020 mol) of C_6F_5OH in 20 mL of ethanol at room temperature. Stirring was terminated after 25 min, and after removal of the ethanol under reduced pressure (50 °C/6 kPa) using a rotary evaporator, the resulting white solid was dried under vacuum at 150 °C for 1 hour.

2.2. 2032-coin cell evaluations

The electrochemical evaluation method for *Section 2.2* to *2.5* was the same as in a previously reported work [24]. The cell performance was evaluated using 2032 type coin cells (1st charge capacity: 2.3mAh). The cathode electrode was comprised of $LiNi_{0.5}Co_{0.2}Mn_{0.3}O_2$ (NCM523) as the active material, and the mixture ratio of NCM523:acetylene black (AB):polyvinylidene fluoride (PVdF) = 92:5:3. The cathode bulk load was 95 g m^{-2} and the press density was 2.5 g cm^{-3}. The anode electrode was comprised of natural graphite (NG) as the active material, and the mixture ratio of NG:styrene butadiene rubber (SBR):carboxymethyl cellulose (CMC) = 98:1:1. The cathode was coated on aluminum foil and the anode was coated on copper foil. The anode bulk load was 55 g m^{-2} and the press density was 1.45 g cm^{-3}. Both electrode sheets were manufactured by the Furukawa Battery Co., Ltd. In this paper, we call the positive electrode the cathode and the negative electrode the anode.

The NCM523/NG full cell was constructed with a Ø14-mm cathode electrode and a Ø15-mm anode electrode. A Ø19-mm, 20-μm thick triple-layer PP/PE/PP separator made by Ube Maxell Co., Ltd., was placed between both electrodes, and a Ø16-mm glass fiber paper, Whatman GF/A made by Cytiva, was also placed between the separator and the cathode electrode. The construction of coin cell is shown in Fig. S1. The N/P ratio of the full cell was defined as the ratio of the initial anode charge capacity to the initial cathode charge capacity, and the N/P ratio was approximately 1.3 for all cells. The electrolytes were 1 M $LiPF_6$ PC/DMC=1/2 (v/v) and 1 M $LiPF_6$ EC/DMC=1/2 (v/v), and the

amount of the injected electrolyte was approximately 0.2 cm^3.

The cell performances were evaluated using an ACD-M01A charge-discharge system (ASKA Electronic Co., Ltd.) The cycling test of the NCM523/NG full cell was performed at 25 °C, 1 C rate (1 $C = 2.3$ mA), from 4.2 V-cccv to 3.0 V-cc.

2.3. Coin cell impedance

The coin cell impedance evaluation of the NCM523/NG full cells was performed using a SP-150 potentiostat (Bio-Logic Science Instruments, Ltd.) at 25 °C, 50 % SOC (50 % charged at 6th cycle), and 10 mV amplitude at frequencies ranging from 500 KHz to 0.01 Hz.

2.4. Reductive decomposition potential

Cyclic voltammetry (CV) to investigate the reductive decomposition potential of the additives was performed using a SP-150 potentiostat (Bio-Logic Science Instruments, Ltd.) at 25 °C with a sweep rate of 0.1 mV s^{-1} in the potential range of 0.005–2.0 V using a NG/Li/Li (w/c/r) three-electrode glass cell. A stainless-steel grid welded to a stainless-steel plate was used as the working electrode, and the NG anode electrode was pressed on this grid.

2.5. Oxidative decomposition potential

Linear sweep voltammetry (LSV) to investigate the oxidative decomposition potential of the additives was performed using a SP-150 potentiostat (Bio-Logic Science Instruments, Ltd.) at 25 °C, at the sweep rate of 5 mV s^{-1} from the open-circuit voltage (OCV) to the oxidation side until the current value reached 100 mA using an AB/Li/Li (w/c/r) three-electrode glass cell. The oxidative decomposition potential was defined as the value at which the current value reached 0.4 mA g^{-1}. By using AB, a typical carbon commonly used as a conductive material for the NCM523 cathode electrode, as the working electrode, the current density was increased making it easier to clearly measure the oxidative decomposition potential of the additives. A 5 % PVdF solution dissolved in N-methyl-2-pyrrolidone (NMP) (#9305 made by the KUREHA Corporation) was mixed with AB (DENKA BLACK Li-400 made by the Denka Co., Ltd.) to give a mass ratio of AB:PVdF = 70:30. The slurry was coated on aluminum foil and dried at 70 °C. After roll pressing, the electrode was welded on an 0.5-mm thick aluminum plate to prepare the AB working electrode. The weight of the AB + PVdF was about 0.59 mg cm^{-1} or 0.41 mg AB cm^{-2}.

2.6. Graphite surface analysis

The graphite anode surface was observed by scanning electron microscopy (SEM) and X-ray photoelectron spectroscopy (XPS). The analysis samples were prepared by disassembling the NCM523/NG full cells after the fifth discharge and removing the anode electrodes. Prior to the SEM and XPS measurements, the anode electrodes were washed twice with DMC to remove any electrolyte residue. A JSM-7001F manufactured by JEOL Ltd. was used for the SEM observations, and an ESCA 5600 manufactured by ULVAC-PHI, Inc., was used for the XPS measurements.

The thickness of the SEI was defined as the depth at which the ratio of the carbon atoms to all the elements, excluding the lithium atoms, reached 95 % in the depth profile measured by XPS. Since the boundary between the surface SEI and the graphite anode material is not flat and it is hard to uniformly etch the surface, the carbon atom ratio at the boundary is thought to asymptotically increase near 95 %, so it was defined in this way.

2.7. Computer simulation

Computer simulations were performed at the HF/6–31G(d) level using Gaussian09w software. The resolved structure calculations were performed at charge = −1.

3. Results and discussion

3.1. Additives used in the evaluation

In this work, the methanesulfonate esters with substituents on the benzene ring were evaluated. The compounds used as additives were phenyl methanesulfonate (MSP, Fig. 1(a)), 2-fluorophenyl methanesulfonate (2F, Fig. 1(b)), 3-fluorophenyl methanesulfonate (3F, Fig. 1(c)), 4-fluorophenyl methanesulfonate (4F, Fig. 1(d)), 2,6-difluorophenyl methanesulfonate (26F, Fig. 1(e)), 2,4-difluorophenyl methanesulfonate (24F, Fig. 1(f)), 3,4,5-trifluorophenyl methanesulfonate (345F, Fig. 1(g)), 2,3,4,5,6-pentafluorophenyl methanesulfonate (23456F, Fig. 1(h)), 2-(trifluoromethyl) phenyl methanesulfonate (2CF_3, Fig. 1(m)), 3-(trifluoromethyl) phenyl methanesulfonate (3CF_3, Fig. 1(n)), 4-(trifluoromethyl) phenyl methanesulfonate (4CF_3, Fig. 1(p)), 3,5-bis(trifluoromethyl) phenyl methanesulfonate (35CF_3, Fig. 1(q)), 2-cyanophenyl methanesulfonate (2CN, Fig. 1(r)), 2-nitrophenyl methanesulfonate (2NO_2, Fig. 1(s)), and 2-methoxyphenyl methanesulfonate (2OCH_3, Fig. 1(t)). These additives were compared to fluoroethylene carbonate (FEC, Fig. 1(x))

3.2. Charge-discharge cycling of NCM523/Gr full cell (0.15 M additive amount)

The cycling performance was investigated by specifying the amount of additive in 1 M $LiPF_6$ PC/DMC as 0.15 M. For comparison, 1 M $LiPF_6$ EC/DMC=1/2 without any additive (hereafter referred to as the EC system) and 1 M $LiPF_6$ PC/DMC=1/2 + 0.15 M FEC were used (Fig. 2). The advantage of this method for introducing additives into the PC/DMC electrolytes is that the additive-derived SEI formation capability can be predicted from the initial discharge capacity (mAh g^{-1}). The durability of the additive-derived SEI can also be predicted from the cycling performance (%). We believe that this evaluation method using PC-based electrolytes is a simple and reproducible screening method.

While the EC system had a battery capacity of 140 mAh g^{-1}, the 1 M $LiPF_6$ PC/DMC=1/2 + 0.15 M (1.3 wt %) FEC had only about half that capacity. In 1999, R. McMillan et al. reported that "adding EC to FEC/PC electrolyte reduces irreversible capacity" [25]. This result is similar to our specific condition (1 M $LiPF_6$ PC/DMC=1/2 + 0.15 M FEC) that has no EC solvent. In contrast, in silicon thin-film electrodes, the addition of 3 wt % FEC to the EC system, not PC, has shown to form an SEI with a significantly improved discharge capacity retention and coulombic efficiency [26]. In light of this result, it can be said that when a small amount of FEC, around 0.15 M (1.3 wt %), was added to an EC-free PC-based electrolyte, the ability of the FEC to form an SEI on the graphite anode is not necessarily sufficient.

On the other hand, 1 M $LiPF_6$ PC/DMC without any additive resulted in a zero discharge capacity due to PC solvent decomposition on the graphite anode (Fig. 2a). 1 M $LiPF_6$ PC/DMC + 0.15 M MSP also showed a zero discharge capacity, indicating that no SEI was formed. No additive showed a graphite exfoliation curve in the 1st cycle of charging, and the discharge capacity was zero (Fig. S2). Therefore, to facilitate the reductive decomposition, we considered introducing an electron-withdrawing F group into the phenyl group.

First, comparing the discharge capacities of the 2F, 3F, and 4F structural isomers having one F group introduced at the 300th cycle, they were 93.0 mAh g^{-1}, 49.5 mAh g^{-1}(220th), and 0 mAh g^{-1}, respectively (Fig. 2b). These results indicated that the introduction of one F group to the benzene ring leads to SEI formation, with the F group in the *o*-position being the most effective. Next, we decided to compare 26F and 24F comprised of a double F group. As shown in Fig. 2c, the discharge capacities at the 300th cycle were 135.3 mAh g^{-1} and 107.7 mAh g^{-1}, respectively. Based on these results, it was found that all of the

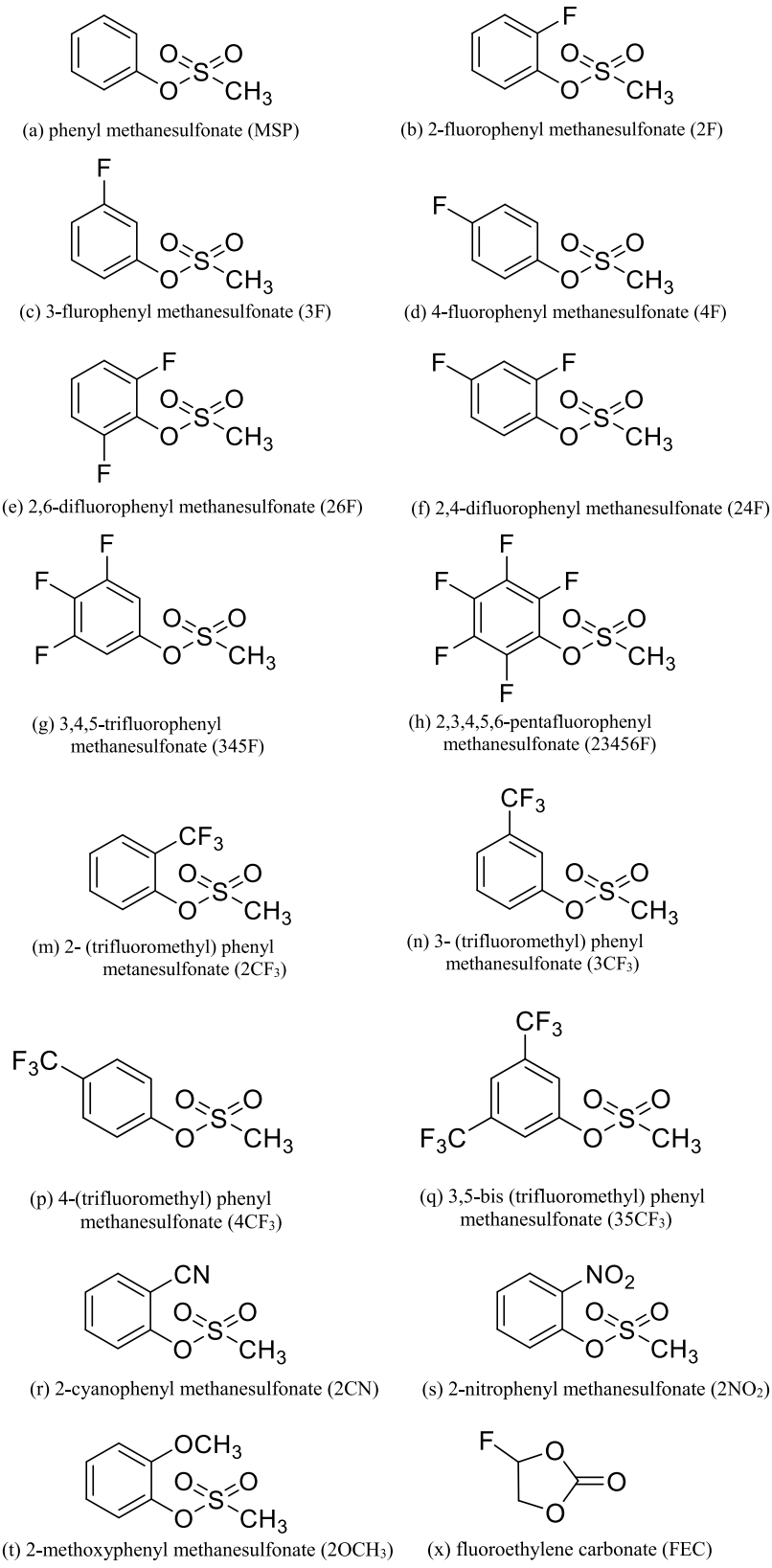

Fig. 1. Structures of the evaluated additives.

cycling performances were better than those of 2F with a single F group, especially, 26F with a double F group in the *o*-position showed a discharge capacity equivalent to that of the EC system. This result also suggested that the *o*-positioned F group is the most effective for reductive decomposition on the graphite anode. This could be explained by the electron withdrawing F group being closer to the CH_3SO_3 group when at the *o*-position. We further compared 345F, which has a triple F group but no F group in the *o*-position with 23456F where all five

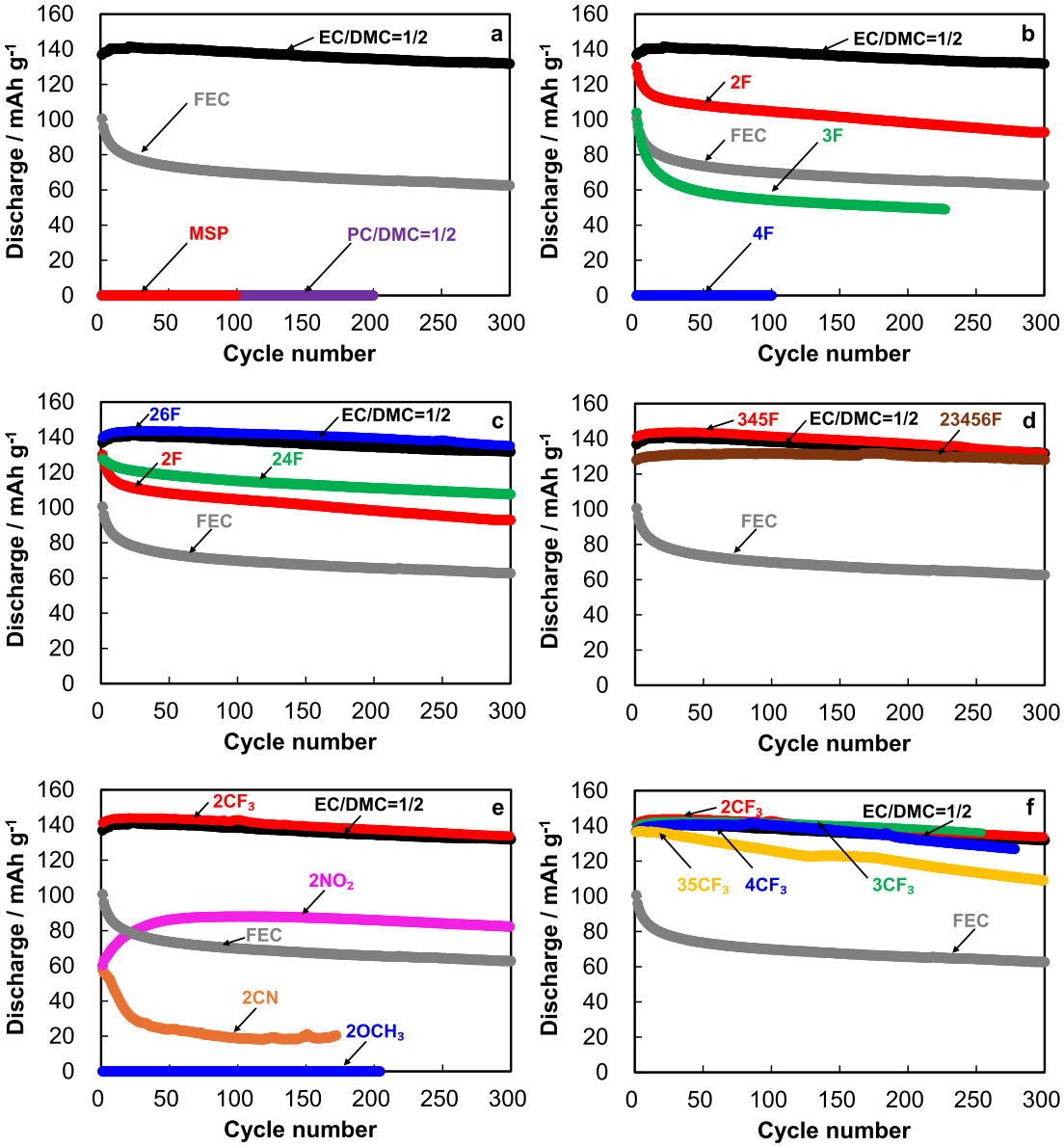

Fig. 2. 1C rate cycling performance of NCM523/NG full-cell with 1 M $LiPF_6$ PC/DMC=1/2 (v/v) + 0.15 M additives. The reference is 1 M $LiPF_6$ EC/DMC=1/2 (v/v).

hydrogen atoms in the benzene ring are substituted with F groups. As shown in Fig. 2d, the discharge capacities at the 300th cycle were 132.1 mAh g^{-1} and 128.3 mAh g^{-1}, respectively. These results indicated that when the number of F groups is increased to three, even 345F, which has no F group in the *o*-position, it exhibits a discharge capacity equivalent to that of the EC system. In addition, although 23456F exhibited an excellent performance, its capacity was slightly lower than that of the EC system.

The impedance corresponding to the cycling performance of 23456F (0.15 M (3.2 wt %)) in Fig. 2d is shown in blue in Fig. S3. The impedance of 23456F at 5 wt % is shown in green and the impedance of 0.25 wt %, shown later in Fig. 3c for the cycling performance, is shown in red. As can be seen from Fig. S3, the impedance increases with the amount of added 23456F, suggesting that the added amount of 23456F has a subtle effect on the discharge capacity.

We then decided to investigate the effects of substitutions by other electron-withdrawing groups (-CF_3, -CN, -NO_2) or electron-donating groups (–OCH_3 group) in the benzene ring on the cycling performance (Fig. 2e). As the *o*-position for the F group can improve the cycling performance, for other substituents, we first tested them at the *o*-position. The discharge capacity of $2CF_3$ at the 300th cycle was 133.8 mAh g^{-1}, which was equivalent to that of the EC system, while that of 2CN and $2NO_2$ were 19.7 mAh g^{-1}(170th) and 82.3 mAh g^{-1}, respectively. On the other hand, $2OCH_3$ showed no discharge capacity at all and was found to have a zero discharge capacity, similar to the first described MSP. Since $2CF_3$ in the *o*-position showed a good discharge capacity of 133.8 mAh g^{-1}, we decided to investigate $3CF_3$ in the *m*-position and $4CF_3$ in the *p*-position. The discharge capacities of the *m*-position $3CF_3$ and *p*-position $4CF_3$ at the 300th cycle were 133.8 mAh g^{-1} and 137.1 mAh g^{-1}, respectively (Fig. 2f). $2CF_3$, $3CF_3$, and $4CF_3$ showed a typical charge-discharge curve (Fig. S2). This indicated that there is no regioselectivity of the -CF_3 group substituent at the 0.15 M addition level. The discharge capacity of $35CF_3$ with two -CF_3 groups in the *m*- position was 109.1 mAh g^{-1} at the 300th cycle. This indicated that, unlike the F group, increasing the amount of the -CF_3 group has no effect on the discharge capacity.

These results indicated that the introduction of certain substituents to the benzene ring changes the discharge capacity, and that the

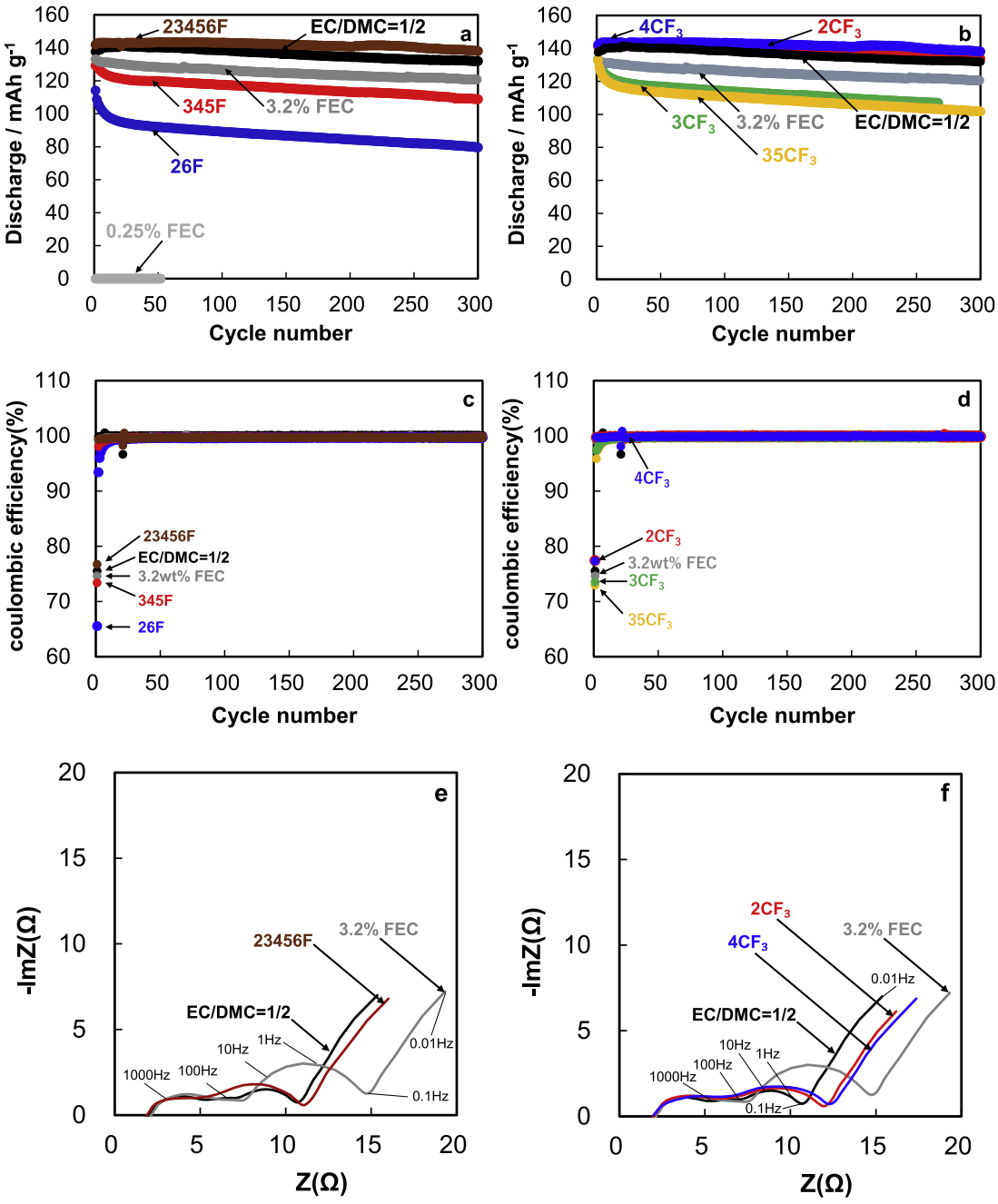

Fig. 3. NCM523/NG full-cell 1C rate cycling performance (a,b), coulombic efficiency (c,d) and corresponding impedancemeasurements (e,f) at 50 % SOC (6th cycle) with 1 M $LiPF_6$ PC/DMC=1/2 (v/v) + 0.25 wt % additives. Reference is 1 M $LiPF_6$ EC/DMC=1/2 (v/v).

introduction of electron-withdrawing groups, such as the F and CF_3 groups, to the phenyl group is effective for SEI formation.

3.3. Charge-discharge cycling of NCM523/Gr full cell (0.25 wt % additive amount)

As mentioned in the Introduction, if the additive amount could be reduced there would be significant advantages for LIBs in EVs, such as reduced impedance and prevention of electrolyte depletion. Therefore, we decided to reduce the amount of the additive at once to 0.25 wt %, which is less than one-tenth, from the amount of additive that showed a good cycling performance at 0.15 M described in *Section 3.2*.

First, the discharge capacities of FEC, 26F, 345F, and 23456F with F groups at the 300th cycle were 0 mAh g^{-1}, 79.7 mAh g^{-1}, 108.9 mAh g^{-1}, and 138.1 mAh g^{-1}, respectively (Fig. 3a). On the other hand, it was found that FEC must be added at 3.2 wt % or more to obtain a discharge capacity equivalent to that of the EC system, and a significant difference in the discharge capacity at the 300th cycle is apparent. Compared to the discharge capacity of FEC, the capacities of 26F and 345F were reduced by approximately 40 % and 20 %, respectively, versus that of the EC system. Only 23456F was found to maintain an excellent discharge capacity equivalent to that of the EC system. Based on these results, it was found that when more F groups are substituted, a greater amount of addition can be reduced. The reason why the discharge capacity of 23456F was about 10 % lower than that of 23456F in the previous Fig. 2d is thought to be that the high reductive decomposition rate of 23456F caused an excess SEI, which increased the impedance and slightly lowered the discharge capacity.

Next, the discharge capacities of the $2CF_3$, $3CF_3$, and $4CF_3$ with CF_3 groups were 133.9 mAh g^{-1}, 107.7 mAh g^{-1}(250th), and 138.1 mAh g^{-1} at the 300th cycle, respectively (Fig. 3b). The discharge capacities of $2CF_3$ and $4CF_3$ were comparable to those of EC, but only $3CF_3$ showed a capacity decrease of about 20 %. Furthermore, $35CF_3$ with two CF_3 groups in the *m*-position showed a capacity of 101.9 mAh g^{-1}, similar to that of $3CF_3$ with one CF_3 group in the *m*-position. This indicated that the number of substituted CF_3 groups is not related to the SEI formation, and that the *o*- and *p*-positions can maintain the same excellent discharge capacity as the EC system. Despite using the PC-based electrolyte, no cycling performance drop was observed even after 300th cycle, indicating the superior durability of the SEI. Accordingly, the charge-discharge efficiencies of the additives shown in Fig. 3a and Fig. 3b are shown in Fig. 3c and Fig. 3d It is clear that all of the additives shown here exhibit excellent charge-discharge efficiencies.

Finally, we compared the cell impedances of FEC, 23456F, $2CF_3$, and $4CF_3$, which showed good cycling performances at a 0.25 wt % addition. The impedances of FEC (3.2 wt %), 23456F, $2CF_3$, and $4CF_3$ were 15 Ω, 11.2 Ω, 12.2 Ω, and 12.5 Ω, respectively, indicating that the impedance of 23456F, $2CF_3$, and $4CF_3$ can be reduced by about 20–30 % compared to FEC (Fig. 3e,f). The reason for this may be that the formed SEI is thinner because the amount added is only one thirteenth of a percent that of FEC, which improves the lithium-ion permeability. The C-rate (1C, 2C, 5C) properties of the 1 M $LiPF_6$ PC/DMC=1/2 + additives are shown in Fig. S4. The addition of the 0.25 wt % 23456F or 0.25 wt % $4CF_3$ to the PC-based electrolyte resulted in rate characteristics (5C/1C rate) equivalent to the reference EC/DMC=1/2.

3.4. Reductive decomposition potential

The reductive decomposition potential of each additive was investigated using graphite as the working electrode. The 1 M $LiPF_6$ EC/DMC=1/2 (v/v) was used as the electrolyte, and 0.15 M of each additive was included. The value of the reductive decomposition potential of the additive was defined as the peak top.

First, the reductive decomposition potential of 1 M $LiPF_6$ EC/DMC=1/2 (v/v) was 0.63 V. The 4F (0.64 V) and MSP (0.63 V) with zero discharge capacities were also comparable, suggesting that they do not form an SEI (Fig. 4a). One could assume that the 4F and MSP reductive decomposition peaks overlap with the EC. However, since the intensity of the reductive decomposition peaks is comparable to that of the EC system, it was more correct to assume that they do not form an SEI. Therefore, in the PC-based electrolyte, MSP and 4F are considered to have zero discharge capacities. On the other hand, the reductive decomposition potentials of 2F and 3F were 0.74 V and 0.73 V, respectively, about 0.1 V higher than that of the EC system (0.63 V), suggesting that they form an SEI before the EC decomposition.

Since the reductive decomposition potential of 23456F was 1.29 V, about 0.66 V higher than the potential of the EC system (0.63 V), suggesting that 23456F can form an SEI much earlier than the decomposition of the PC solvent, thus showing a good cycling performance. As the number of F substitutions increased (24F, 26F, 345F, and 23456F), the reductive decomposition potential increased (Fig. 4b). In addition, 23456F with substitutions by five fluorines was found to have a higher reductive decomposition current. This means that the SEI formation occurs faster and the decomposition amount is greater for 23456F.

Next, the reductive decomposition potentials of $2CF_3$ and $4CF_3$ with CF_3 groups were 0.96 V and 0.96 V, respectively, about 0.3 V higher than that of the EC system (0.63 V) (Fig. 4c). Furthermore, their decomposition potentials are about 0.2 V higher than those of the *o*-position 2F (0.74 V) and *p*-position 3F (0.73 V), which may indicate a good cycling performance since they form an SEI earlier than 2F and 3F. On the other hand, the reductive decomposition potential of $3CF_3$ in the *m*-position was 0.88 V, about 0.1 V lower than those of $2CF_3$ and $4CF_3$, suggesting that the cycling performance was slightly inferior to $2CF_3$ and $4CF_3$. The reductive decomposition potential of FEC (0.85 V) is also about 0.1 V lower than those of $2CF_3$ (0.96 V) and $4CF_3$ (0.96 V) and slightly lower than that of the *m*-position $3CF_3$ (0.88 V). In addition, the amount of the reductive decomposition of FEC is less than those of $2CF_3$, $3CF_3$, and $4CF_3$, hence it is expected that the equivalent SEI cannot be formed without a higher addition amount. This is related to the aforementioned FEC's ability to form an SEI that is not always sufficient. $35CF_3$ with two CF_3 groups showed a higher reductive decomposition potential and increased reductive decomposition current, similar to fluorine (Fig. 4c). However, the cycling performance of $35CF_3$ was worse than that of $3CF_3$ (Fig. 3b). Therefore, the substitution positions at the *o*- and *p*-positions may also be important factors in improving the cycling performance.

Furthermore, the reductive decomposition potentials of the other electron-withdrawing groups, 2CN and $2NO_2$, were 1.24 V and 2.28 V, respectively (Fig. 4d). All of these additives were found to have decomposition potentials of 1 V or higher. However, focusing on the decomposition quantity of these additives, it was found to be much more than twice that of 23456F. Therefore, the -CN and -NO_2 groups directly undergo electrochemical reactions, which may have adversely affected the battery performance. On the other hand, the reductive decomposition potential of the electron-donating group, 2OCH3, was 0.64 V, equivalent to that of the EC system (0.63 V). Therefore, as with the aforementioned 4F and MSP, the PC-based electrolyte is considered to have a zero discharge capacity because it does not form the SEI.

Additives that exhibit good cycling performances, such as 23456F and CF_3, must have a reductive decomposition potential near 1 V away from the decomposition potential of EC. The structure of the substituents also needs to not cause any electrochemical side reactions.

3.5. Oxidative decomposition potential

The oxidation potential of each additive was then investigated using AB as the working electrode. The electrolyte was 1 M $LiPF_6$ EC/DMC=1/2 (v/v), the same as the reductive decomposition potential, and 0.15 M of each additive was included. The value of the oxidative decomposition potential of the additive was defined as the current value when 0.4 mA g^{-1} was reached.

First, the potential of 1 M $LiPF_6$ EC/DMC=1/2 (v/v) without additives was 5.03 V. The oxidative decomposition potentials of 2F (4.94 V) or 3F (4.96 V) and 4F (4.97 V) or MSP (4.97 V), which had a zero capacity, were nearly identical and slightly lower than those of the EC system (5.03 V) (Fig. 4e). The oxidative decomposition potential of 23456F, in which all the hydrogens in the benzene ring were replaced by fluorine, is 5.01 V, which is slightly better than the 4.97 V of MSP (Fig. 4f). Since they all have approximately the same oxidation potential as the EC system, oxidative decomposition on the cathode side is not as likely to occur as reductive decomposition on the anode side. Next, the oxidation potentials of $2CF_3$, $3CF_3$, and $4CF_3$ with CF_3 groups were 5.01 V, 5.03 V, and 5.01 V, respectively (Fig. 4*g*). Since all of them have oxidation potentials equivalent to that of FEC (5.03 V), it can be said that oxidative decomposition on the cathode side does not occur as easily as reductive decomposition on the anode side.

Furthermore, the oxidative decomposition potentials of the other electron-withdrawing groups, 2CN and $2NO_2$, were 4.92 V and 5.03 V, respectively (Fig. 4h). Since both have the same oxidation potential as that of the EC system, it can be said that the oxidative decomposition on the cathode side does not occur as easily as the reductive decomposition on the anode side. On the other hand, the oxidation potential of the electron-donating group, $2OCH_3$, was 4.49 V. This is about 0.5 V lower than that of the EC system, suggesting that oxidative decomposition more easily occurs on the cathode side.

Based on these oxidative decomposition potential data, it is clear that the main decomposition of 23456F and CF_3 is used for SEI formation on the anode side with little decomposition occurring on the cathode side. The decomposition potentials observed are summarized in Table 1.

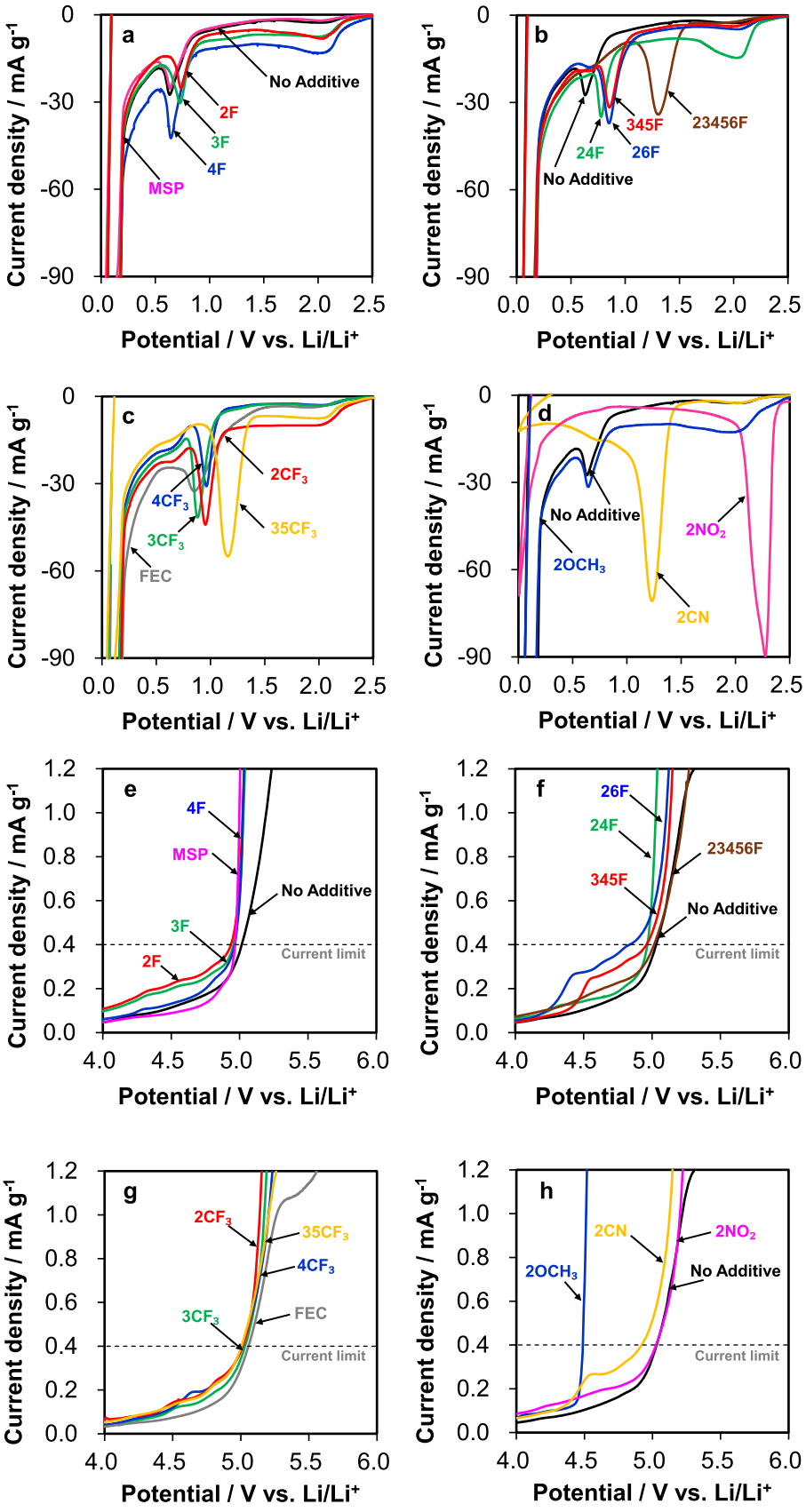

Fig. 4. NG/Li/Li three-electrode glass cell cyclic voltammetry measurement at 0.1 mV s^{-1}, 1st cycle (a-d), and linear sweep voltammetry of AB/Li/Li three-electrode glass cell measurement at 5 mV s^{-1}, 1st cycle (e-h) measurement with 1 M $LiPF_6$ EC/DMC=1/2 (v/v) + 0.15 M additives.

Table 1
Summary of the reductive and oxidative decomposition potentials.

Abbre-viation	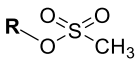	Dec. potential (V vs. Li/Li^+)	
	R	Red.	Ox.
MSP	phenyl	0.63	4.97
2F	2-fluorophenyl	0.74	4.94
3F	3-fluorophenyl	0.73	4.96
4F	4-fluorophenyl	0.64	4.97
24F	2,4-difluorophenyl	0.78	4.97
26F	2,6-difluorophenyl	0.86	4.84
345F	3,4,5-trifluorophenyl	0.86	4.96
23456F	2,3,4,5,6-pentafluorophenyl	1.29	5.01
$2OCH_3$	2-methoxyphenyl	0.64	4.49
$2NO_2$	2-nitrophenyl	2.28	5.03
2CN	2-cyanophenyl	1.24	4.92
$2CF_3$	2-(trifluoromethyl)phenyl	0.96	5.01
$3CF_3$	3-(trifluoromethyl)phenyl	0.88	5.03
$4CF_3$	4-(trifluoromethyl)phenyl	0.96	5.01
$35CF_3$	3,5-bis(trifluoromethyl)phenyl	1.16	5.00
FEC	fluoroethylene carbonate	0.85	5.03
Ref.	1 M $LiPF_6$ EC/DMC=1/2	0.63	5.03

3.6. Graphite surface analysis

SEM images of the graphite surfaces of 23456F and $4CF_3$, having the best cycling performances at the 0.25 wt % additive level were compared with that of FEC (Fig. 5, upper part). The graphite interface of FEC had a large grain size and was uneven. On the other hand, 23456F had a smaller grain size and densely adhered to the surface. In addition, $4CF_3$ had an extremely small grain size and was smooth with few bumps and indentations. Since the surface morphologies of FEC, 23456F, and $4CF_3$ by SEM are clearly different, and the SEI quality may be different, we next analyzed the SEI using XPS.

XPS was then used to measure the depth profile of the SEI (Fig. 5, middle part). The measured SEI thickness is intended to compare the relative SEI thickness between additives and is not absolute. Therefore, the thickness of the SEI by the depth profile was defined as the SEI thickness at the point where the concentration of carbon atoms, excluding lithium atoms, reached 95 % of the total, as described in *Section 2.5*.

The SEI thicknesses of FEC, 23456F, and $4CF_3$ were all about 20 nm with no meaningful difference. In addition, Figs. 3e and 3f show that FEC had a higher impedance than 23456F and $4CF_3$. Thus, even though the thickness of the SEI of 23456F is similar to that of FEC, it is denser than that of FEC. Despite their higher density, the impedances for 23456F and $4CF_3$ are lower than that of FEC, therefore, their SEI is more permeable to lithium ions. The amount of the reductive decomposition of the FEC in Fig. 4 was less than that of 23456F and $4CF_3$. Considering that the added amount of FEC is 3.2 wt %, which is about 13 times higher than the other additives of 0.25 wt %, the reductive decomposition rate of FEC is low. Furthermore, the C element ratios of the top surface were FEC: 47.6 %, 23456F: 55.0 %, and $4CF_3$: 57.4 %. The C element ratios of 23456F and $4CF_3$ are 10 % higher than those of FEC, suggesting that they form a carbon-rich SEI. Next, the F element ratios were 9.0 %, 3.0 %, and 3.6 % for FEC, 23456F, and $4CF_3$, respectively. The F element ratio was high for FEC, suggesting that it forms a fluorine-rich SEI. The most characteristic feature was the S element ratio, which was 23456F:0.5 % and $4CF_3$:0.4 %. These results suggest that the reason why the impedances of 23456F and CF_3 were lower than that of FEC can be attributed to the fact that the SEI is rich in organic matter and contains the S element.

The C1s, F1s, and S2p spectra of the anode surface were measured by XPS (Fig. 5, lower part). First, in the C1s spectra of 23456F and $4CF_3$, more C—C-derived peaks appeared than in FEC, supporting the formation of an organic-rich film. In both cases, a CO_3-derived peak was observed around 290 eV for 23456F and $4CF_3$. In Figs. 4a and 4b, a very small decomposition peak was present around the EC decomposition potential. This suggests that the PC solvent decomposition products exist only on the topmost surface. That is why the C1s spectra showed a CO_3-derived peak only until a 3-nm thickness. Next, the F1s spectra of FEC, 23456F, and $4CF_3$ all showed a LiF-derived peak around 685 eV. In particular, FEC has a strong LiF peak intensity, and the LiF peak is even seen inside the graphite, suggesting that the inorganic-rich SEI due to the fluorine atom reduces the lithium-ion permeability. Furthermore, the S2p spectra show peaks around 169 eV only for 23456F and $4CF_3$. This indicated that the decomposition products derived from the CH_3SO_3 groups are deposited on the graphite anode in both cases, and the peak around 169 eV is presumed to be CH_3SO_3Li or Li_2SO_4, which may have the effect of promoting the lithium-ion permeability of the SEI. In summary, 23456F and $4CF_3$ may form a thin SEI with organic-rich sulfur oxides on the top surface, thus improving the lithium-ion permeability and reducing the SEI impedance. This study has revealed that, depending on the additive structure, the thickness and quality of the SEI have a significant impact on the battery performance.

3.7. Predicted decomposition mechanism

Finally, the expected decomposition mechanism of 23456F is shown in Fig. 6(1). Additive decomposition mechanisms were estimated using the computer simulation Gaussian09w (Fig. S5). However, in this work, we decided to use the HF method, which does not take into account electron correlations, in order to give priority to estimating the rough decomposition mechanism. We also consulted the literature on the decomposition mechanisms of PMS with propargylic groups [16], VC with vinyl groups [27], and FEC [28]. The 2F, 3F, 23456F, and $4CF_3$ predicted conformations decomposed into radicals and methanesulfonate anions by the "charge = −1″ reductive decomposition state. In contrast, MSP and 4F did not decompose even in the "charge = −1" reductive decomposition state. These results are in good agreement with the discussion about the experimental data for the reductive decomposition potentials in *Section 3.4*.

Based on these findings, we considered routes 1A and 1B as the decompositions of 23456F. First, when 23456F is cleaved in route 1A, a decomposed product containing CH_3SO_3Li and a pentafluorophenyl group is formed, as reported in the referenced literature. The decomposed product containing a pentafluorophenyl group may be pentafluorobenzene (1X) or coupled to form perfluorobiphenyl (1Y). Second, although not reported in the literature, in the case of cleavage during route 1B, there is the case of a methanesulfonyl radical (CH_3SO_2 •) and Li-OC_6F_5 (1Z). Therefore, we actually added 1X:0.012 M, 1Y:0.006 M, and 1Z:0.012 M of the expected decomposition products to 1 M $LiPF_6$ PC/DMC=1/2 (v/v), then compared their cycling performances (Fig. 6 (1)). The results showed that 1X exhibited a cycling performance equivalent to 23456F, while 1Y and 1Z had lower capacities, suggesting that 23456F was reductively decomposed in route 1A to form CH_3SO_3Li and 1X, and that 1X contributed to the SEI formation.

The expected decomposition mechanism of $4CF_3$ is similarly shown in Fig. 6(2). Based on the results of 23456F, we considered that $4CF_3$ would be similarly reductively decomposed during route 2A. After cleavage during route 2A, the decomposed product contains CH_3SO_3Li and a phenyl group which may be trifluoromethyl benzene (2X) or 4,4-bis (trifluoromethyl) biphenyl (2Y), where 2X is coupled. Therefore, we actually compared the cycling performance of 1 M $LiPF_6$ PC/DMC=1/2 (v/v) with 2X: 0.012 M and 2Y: 0.006 M of the respective expected decomposition products (Fig. 6(2)). The results showed that the discharge capacities of both were zero, suggesting that the decomposition mechanisms of 23456F and $4CF_3$ are completely different, and that $4CF_3$ probably forms polymers or oligomers. However, at this stage, no direct evidence has been obtained to support this expectation, and further research is needed.

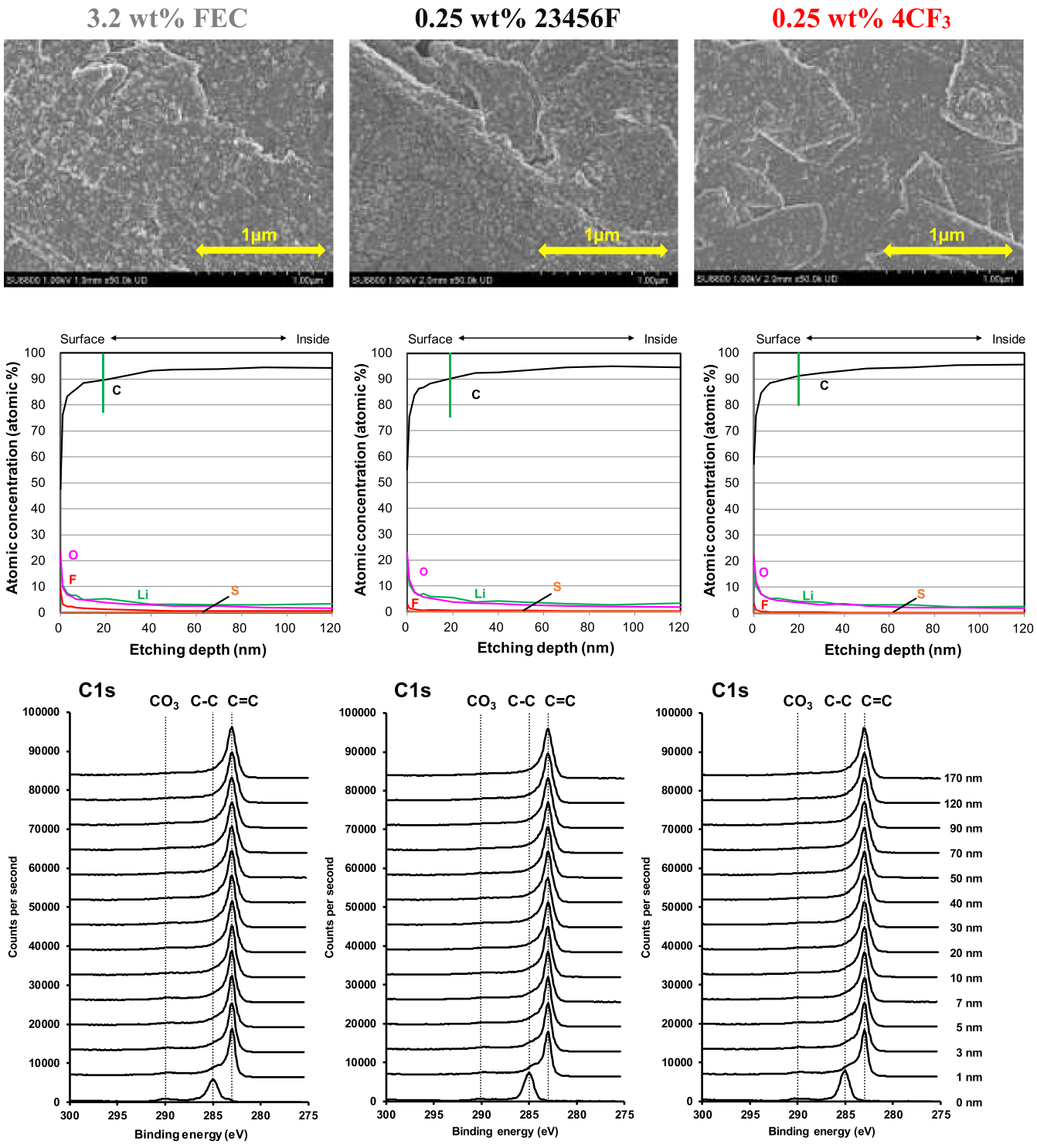

Fig. 5. SEM images, XPS depth profile, and XPS C1s, F1s, and S2p spectrum of the graphite anode surface at the 5th discharge cycled in 1 M $LiPF_6$ PC/DMC=1/2 (v/v) + additives.

4. Conclusion

Among the methanesulfonates with substituents on the benzene ring, 4-(trifluoromethyl) phenyl methanesulfonate ($4CF_3$) was found to be an excellent SEI forming electrolyte additive, comparable to 2,3,4,5,6-pentafluorophenyl methanesulfonate (23456F). The amount of $4CF_3$ and 23456F added to the electrolyte was a very low (0.25 wt %), much lower than the optimum amount of 3.2 wt % for FEC. The results suggest a low cell impedance and excellent lithium-ion permeability.

This work showed that what is important in the structural design of additives is the timing of the SEI formation and the quality of the SEI. First, the timing of the SEI formation can be controlled by regioselectively introducing electron-withdrawing substituents, such as $4CF_3$ and 23456F, to control the potential for the SEI formation. Second, the quality of the SEI was found to be due to the structure of the ester moiety of the methanesulfonate ester.

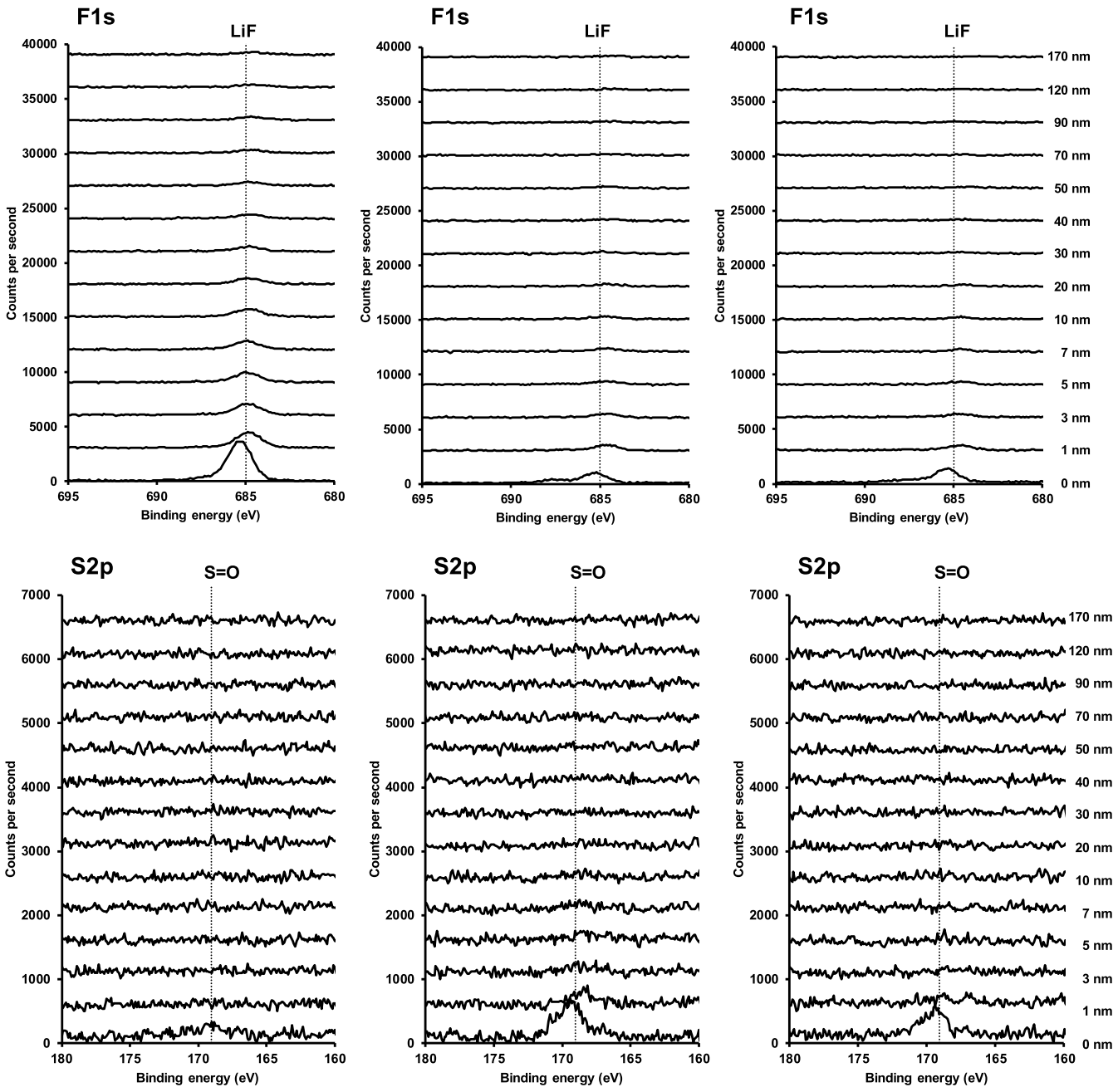

Fig. 5. (*continued*).

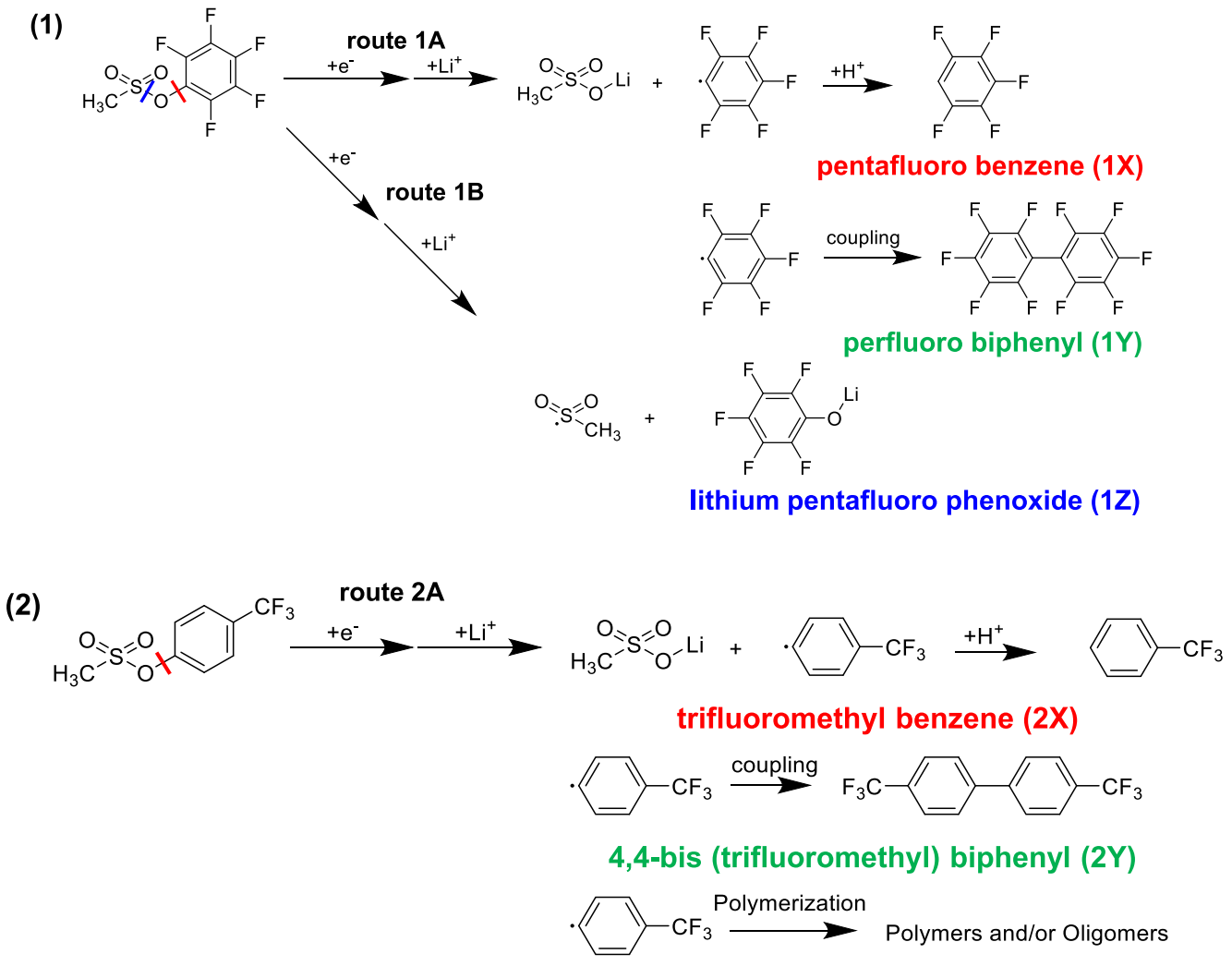

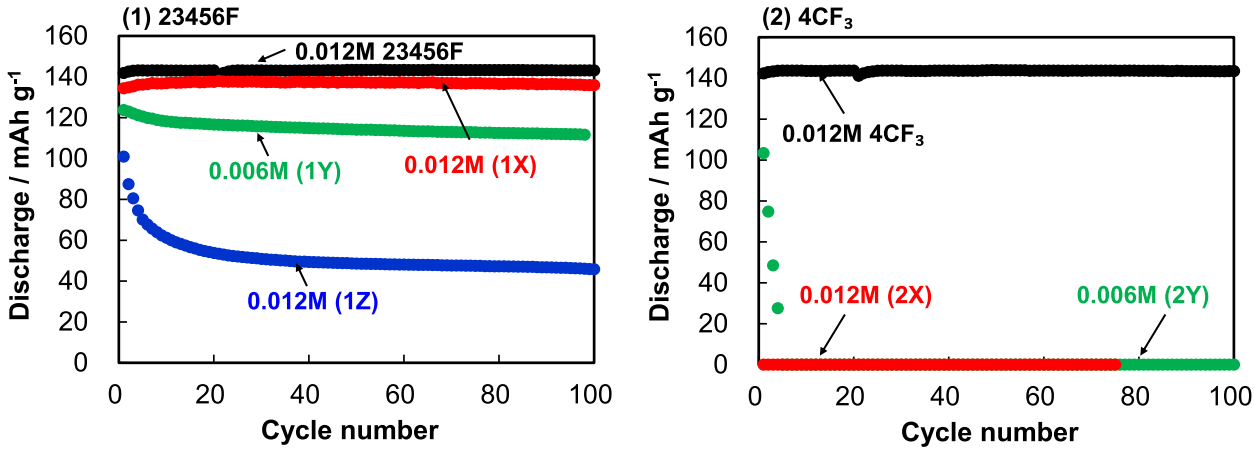

Fig. 6. Proposed decomposed mechanism of 23456F and $4CF_3$ in graphite anode and NCM523/NG full-cell 1C rate cycling performance with 1 M $LiPF_6$ PC/DMC=1/2 (v/v) + 0.012 M or 0.006 M expected decomposition products.

My intuition, based on many years of research on electrolyte additives, is that in order to find additives that work at lower dosages than 0.5 wt %, we should pursue "dense SEI" with an excellent lithium-ion permeability. It is necessary to consider in advance what kind of alkyl inorganic salt will be formed after the decomposition of the additive and what kind of resonance structure the organic polymer compound should contain. Thus, "reverse synthesis" from the post-decomposition structure will be useful for additive design. Although analysis of the electrode interface after additive decomposition is complicated and difficult, we expect that the new findings about $4CF_3$ and 23456F from this work will contribute to the further improvement of new SEI forming additives that can replace FEC.

CRediT authorship contribution statement

Keitatsu Miura: Writing – review & editing, Writing – original draft, Investigation, Data curation. **Yanko Marinov Todorov:** Writing – review & editing, Writing – original draft, Validation, Data curation. **Masaki Deguchi:** Writing – review & editing, Writing – original draft. **Koji Abe:** Writing – review & editing, Writing – original draft, Supervision, Methodology, Investigation, Conceptualization.

Declaration of competing interest

The authors declare that they have no known competing financial interests or personal relationships that could have appeared to influence the work reported in this paper.

Supplementary materials

Supplementary material associated with this article can be found, in the online version, at doi:10.1016/j.electacta.2025.147054.

Data availability

Data will be made available on request.

References

[1] H. Yoshitake, in: Battery and Power Supply in Techno-Frontier Symposium F5-3, Japan Management Associates, Makuhari, 1999.
[2] K. Abe and H. Yoshitake, *Electrochemistry*, 72, 520 (2004). https://doi.org/10.5796/electrochemistry.72.519.
[3] S.S. Zhang, J. Power Sources 162 (2006) 1379, https://doi.org/10.1016/j.jpowsour.2006.07.074.
[4] H. Yoshitake, *Lithium-ion batteries* (Modern Aspects of Electrochemistry, 58), in: M. Edition, R.J. Yoshio, A.Kozawa Brodd (Eds.), Chapter 19 Functional Electrolytes Specially Designed For Lithium-Ion Batteries, Springer, New York, 2009, https://doi.org/10.1007/978-0-387-34445-4_19.
[5] Edition K. Abe, *Electrolytes for lithium and lithium-ion batteries* (Modern Aspects of Electrochemistry, 58), in: T.R. Jow, K. Xu, O. Borodin, M. Ue (Eds.), Chapter 3 Nonaqueous Electrolytes, and Advances in Additives, Springer, New York, 2014, https://doi.org/10.1007/978-1-4939-0302-3_3.
[6] A.M. Haregewoin, A.S. Wotango, Bing-Joe Hwang, Energy Environ. Sci. 9 (2014) 1955, https://doi.org/10.1039/C6EE00123H.
[7] K. Xu, Chem. Rev. 104 (2004) 4303, https://doi.org/10.1021/cr030203g, h tt ps://pubs.acs.org/doi/.
[8] K. Xu, Chem. Rev. 114 (2014) 11503, https://doi.org/10.1021/cr500003w.
[9] P. Verma, P. Maire, P. Novák, Electrochim. Acta 55 (2010) 6332–6341, https://doi.org/10.1016/j.electacta.2010.05.072.
[10] V.A. Agubra, J.W. Fergus, J. Power Sources 268 (2014) 153–162, https://doi.org/10.1016/j.jpowsour.2014.06.024.
[11] C. Wang, H. Nakamura, H. Komatsu, M. Yoshio, H. Yoshitake, J. Power Sources 74 (1998) 142, https://doi.org/10.1016/S0378-7753(98)00017-2.
[12] S.-K. Jeong, M. Inaba, R. Mogi, Y. Iriyama, T. Abe, Z. Ogumi, Langmuir 17 (2001) 8281, https://doi.org/10.1021/la015553h, h t t ps://pubs.acs.org/doi/.
[13] K. Abe, H. Yoshitake, T. Kitakura, T. Hattori, C. Wang, M. Yoshio, Electrochim. Acta 49 (2004) 4613, https://doi.org/10.1016/j.electacta.2004.05.016.
[14] K. Abe, T. Hattori, K. Kawabe, Y. Ushigoe, H. Yoshitake, J. Electrochem. Soc. 154 (2007) A810, https://doi.org/10.1149/1.2746570.
[15] K. Abe, T.H. K.Miyoshi, Y. Ushigoe, H. Yoshitake, J. Power Sources 184 (2008) 449, https://doi.org/10.1016/j.jpowsour.2008.03.037.
[16] K.C. Högström, S. Malmgren, M. Hahlin, H. Rensmo, F. Thebault, P. Johansson, K. Edström, J. Phys. Chem. C 117 (2013) 23476–23486, https://doi.org/10.1021/jp4045385, ht tp s://pubs.acs.org/doi/full/.
[17] K.C. Högström, M. Hahlin, S. Malmgren, M. Gorgoi, H. Rensmo, K. Edström, J. Phys. Chem. C 118 (24) (2014) 12649–12660, https://doi.org/10.1021/jp502732j, ht tp s://pubs.acs.org/doi/pdf/.
[18] R. Wang, Z. Wang, X. Li, H. Zhang, Electrochim. Acta 241 (2017) 208–219, https://doi.org/10.1016/j.electacta.2017.04.125.
[19] X. Gao, J. You, L. Deng, B. Zhang, Y. Li, W. Wang, J. Mater. Chem. A 12 (37) (2024) 25211–25221, https://doi.org/10.1039/D4TA04755A.
[20] J. You, L. Deng, S. Meng, Y. Li, L. Liu, W. Wang, Electrochim. Acta 515 (2025) 145720, https://doi.org/10.1016/j.electacta.2025.145720.
[21] K. Abe, T. Kuwata, T. Hattori, Y. Matsumori, US Patent 7297,442 (UBE Co., Ltd.): (2007) applied in 2002.
[22] T. Yang, W. Fan, C. Wang, Q. Lei, Z. Ma, L. Yu, X. Zuo, J. Nan, ACS Appl. Matter. Interfaces. 10 (2018) 31735–33174, https://doi.org/10.1021/acsami.8b04743.
[23] K. Abe, M. Colera, K. Shimamoto, M. Kondo, K. Miyoshi, J. Electrochem. Soc. 161 (2014) A863, https://doi.org/10.1149/2.086405jes.
[24] K. Abe, M. Deguchi, Y.M. Todorov, J. Power Sources 630 (2025) 236046, https://doi.org/10.1016/j.jpowsour.2024.236046.
[25] R. McMillan, H. Slegr, Z.X. Shu, W. Wang, J. Power Sources 81-82 (1999) 20–26, https://doi.org/10.1016/S0378-7753(98)00201-8.
[26] N.-S. Choi, K.H. Yew, K.Y. Lee, M. Sung, H. Kim, S.-S. Kim, J. Power Sources 161 (2006) 1254–1259, https://doi.org/10.1016/j.jpowsour.2006.05.049.
[27] H. Ota, Y. Sakata, A. Inoue, S. Yamaguchi, J. Electrochem. Soc. 151 (2004) A1659, https://doi.org/10.1149/1.1785795.
[28] A.L. Michan, B.S. Parimalam, M. Leskes, R.N. Kerber, T. Yoon, C.P. Grey, B. L. Lucht, Chem. Mater. 28 (22) (2016) 8149–8159, https://doi.org/10.1021/acs.chemmater.6b02282.